2nd International Symposium on Magnetic Beaing
July 12-14, 1990, Tokyo, Japan

Design and Testing of a Flexible Rotor-Magnetic Bearing System

M.HISATANI*, S.INAMI*, T.OHTSUKA*, and M.FUJITA*
*Tamano Laboratory, Mitsui Engineering and Shipbuilding,
3-16-1, Tamahara, Tamano, 706 JAPAN

Abstract

A mechanical model analysis of a flexible rotor is combined with an electrical characteristic modelling of control components of a magnetic bearing system. Eigenvalues and system stability are examined for several control strategies. "Quasi-Colocation Pseudo-Inverse" and "Selective Eigenvalue Move" techniques are presented as practical and effective control design methods. Testing result of the flexible rotor in the form of a transfer function is compared with the calculated value, and the effectiveness of these techniques has been ascertained.

1. Introduction

At the design of a control system of active magnetic bearing supporting a rotating body, degrees of freedom of motion around the center of gravity should only be considered when the object rotor can be treated as a rigid body. The design is rather easy if there are no problems of big unbalance excitation or gyroscopic effect.

On the other hand, if the suspended rotor is flexible and the design speed exceeds the eigen-frequencies of bending modes, the rotor should be treated as a multi-mass body connected by flexible shafts with finite spring constants. The design problem becomes complicated as the number of degrees of freedom increases largely. In addition to such a mechanical modelling for modal analysis or eigenvalue analysis, frequency characteristic of the electrical system of the control circuit should also be taken into account as an element which greatly affects the overall eigenvalues.

The control of flexible rotors has been investigated by many researchers [1-5]. If such techniques as optimal regulator or pole assignment using state feedback can be used, system eigenvalues are arbitrarily designated, bringing as desirable system characteristic as possible. Practically, however, the number of sensors to detect the motion of the rotor is limited, so only a part of the whole states are observed, inhibiting state feed-back. As for the constitution of observer to estimate unknown states, it is very difficult to realize in the actual control circuits as its dimension becomes intolerably large. Therefore, it is necessary to approach the preferable characteristic using output feed-back maintaining stable eigenvalues. Many research works have been performed along this approach. As concrete design methods are proposed Quasi-Modal Control [1] and Pseudo-Inverse [2].

In this paper the total control system is expressed for a practical flexible rotor combining mechanical modelling of lumped mass and beam chain system with electrical modelling considering frequency characteristics. Control system design by output feedback is investigated for several methods, and "Quasi-Colocation Pseudo-Inverse" is presented as an original design method. Also presented is "Selective Eigenvalue Move" method which modifies the fine arrangement of system eigenvalues. Finally the effectiveness of these methods are verified experimentally.

2. Mechanical System Modelling

The rotor is modelled as composed of a few disks with masses and moments of inertia and of connecting shafts without mass. Fig.1 shows k-th shaft section with a variation of section profile bound by two disks of k-th and (k+1)-th. Let shearing force at shaft end be F, bending moment M, inclination θ, and deflection x, then

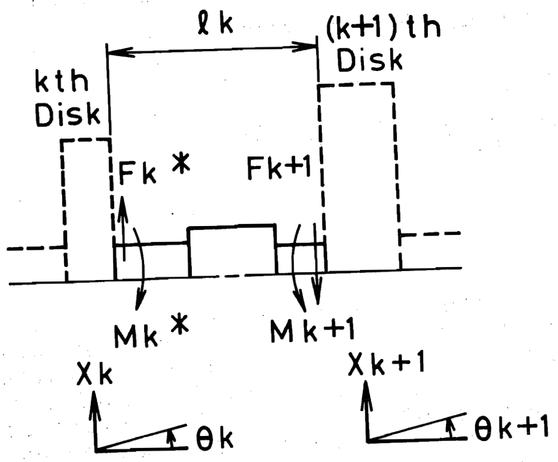

Figure 1 Shaft model

$$\begin{pmatrix} F_{k+1} \\ M_{k+1} \\ \theta_{k+1} \\ x_{k+1} \end{pmatrix} = \begin{pmatrix} 1 & 0 & 0 & 0 \\ l_k & 1 & 0 & 0 \\ a_k & b_k & 1 & 0 \\ c_k & d_k & l_k & 1 \end{pmatrix} \begin{pmatrix} F_k^* \\ M_k^* \\ \theta_k \\ x_k \end{pmatrix} \qquad (1)$$

$$a_k = (l_k^2/2E_kI_k)_a$$
$$b_k = (l_k / E_kI_k)_b$$
$$c_k = (l_k^3/6E_kI_k)_c$$
$$d_k = (l_k^2/2E_kI_k)_d$$

where l_k indicates axial length, E_k modulus of elasticity, and I_k moment of inertia of section. The expression of coefficients $a_k \sim d_k$ with parentheses () indicates that the variation of shaft diameter is considered (see Appendix A), in order to reduce the number of overall degrees of freedom.

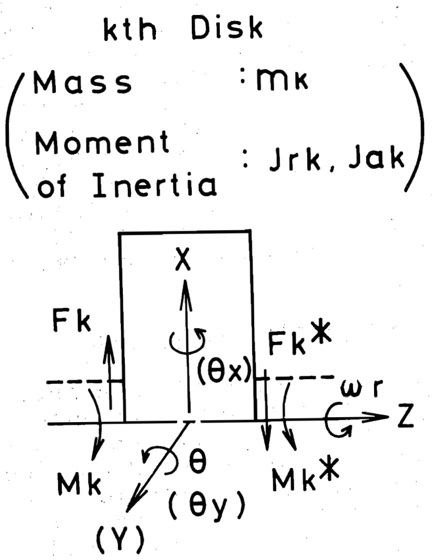

Figure 2 Disk model

From the relation of (1), F and M can be expressed by θ and x as follows;

$$\begin{pmatrix} F_k^* \\ F_{k+1} \\ M_k^* \\ M_{k+1} \end{pmatrix} = 1/\Delta_k \begin{pmatrix} b_kl_k-d_k & d_k & b_k & -b_k \\ b_kl_k-d_k & d_k & b_k & -b_k \\ c_k-l_ka_k & -c_k & -a_k & a_k \\ \left(c_k-l_ka_k+l_k^2b_k-l_kd_k\right) & \left(l_kd_k-c_k\right) & \left(l_kb_k-a_k\right) & \left(a_k-l_kb_k\right) \end{pmatrix} \begin{pmatrix} \theta_k \\ \theta_{k+1} \\ x_k \\ x_{k+1} \end{pmatrix} \qquad (2)$$

$$\Delta_k = a_kd_k - c_kb_k$$

Referring to Fig.2, the equation of motion of k-th disk without internal damping of the rotor is ;

$$m_k \ddot{x}_k = F_k - F_k^* + u_k \qquad (3)$$
$$J_{rk}\ddot{\theta}_k = M_k^* - M_k \qquad (4)$$

where u_k is the bearing reaction force, and J_{rk} is around the radius direction.

Relation (2) is substituted into (3) and (4), with a resulting expression ;

$$\begin{Bmatrix} m_k \ddot{x}_k \\ J_{rk}\ddot{\theta}_k \end{Bmatrix} + \{K_{kij}\} \begin{Bmatrix} x_{k-1} \\ \theta_{k-1} \\ x_k \\ \theta_k \\ x_{k+1} \\ \theta_{k+1} \end{Bmatrix} = \begin{Bmatrix} u_k \\ 0 \end{Bmatrix} \begin{matrix} (i=1,2) \\ (j=1,6) \end{matrix} \qquad (5)$$

where

$$K_{k11} = -b_{k-1}/\Delta_{k-1}$$
$$K_{k12} = (-l_{k-1}b_{k-1}+d_{k-1})/\Delta_{k-1}$$
$$K_{k13} = b_{k-1}/\Delta_{k-1}+b_k/\Delta_k$$
$$K_{k14} = -d_{k-1}/\Delta_{k-1}+(l_kb_k-d_k)/\Delta_k$$
$$K_{k15} = -b_k/\Delta_k$$
$$K_{k16} = d_k/\Delta_k$$
$$K_{k21} = (l_{k-1}b_{k-1}-a_{k-1})/\Delta_{k-1}$$
$$K_{k22} = \{l_{k-1}(b_{k-1}l_{k-1}-d_{k-1}-a_{k-1})+c_{k-1}\}/\Delta_{k-1}$$
$$K_{k23} = (-l_{k-1}b_{k-1}+a_{k-1})/\Delta_{k-1}+a_k/\Delta_k$$
$$K_{k24} = (l_{k-1}d_{k-1}-c_{k-1})/\Delta_{k-1}-(c_k-a_kl_k)/\Delta_k$$
$$K_{k25} = -a_k/\Delta_k$$
$$K_{k26} = c_k/\Delta_k$$

Applying k = 1 ∿ n+1 for the rotor partitioned by n, the equation of motion for the whole system becomes as follow;

$$\underline{M}\,\underline{\ddot{x}} + \underline{K}\,\underline{x} = \underline{L}\,\underline{u} \qquad (6)$$

$\underline{x} = (x_1, \theta_1, x_2, \theta_2, \cdots, x_{n+1}, \theta_{n+1})^T$
$\underline{u} = (u_1, u_2, \cdots)^T$
$\underline{M} = \mathrm{diag}\{m_1, J_{r1}, m_2, J_{r2}, \cdots, m_{n+1}, J_{r(n+1)}\}$
$\underline{K}$: Band matrix composed of K_{kij} (k=1,n+1)
$\underline{L}$: Matrix indicating bearing locations

Underlined letters indicate vectors or matrices, and diag{} means a diagonal matrix.

The natural boundary condition is applied at both ends of the rotor ;

$$F_1 = M_1 = F_{n+1}^* = M_{n+1}^* = 0$$

3. Undamped Mode Analysis

Let $\underline{u}=\underline{0}$ in (6), and eigenvalues of free-free-mode without damping and bearing spring forces are obtained. Substitution of $\underline{x}=\underline{x}_0\exp(j\omega t)$ into (6) yields the form of normal eigenvalue problem ;

$$\underline{A}\ \underline{x} = 1/\omega^2\ \underline{x} \quad ; \quad \underline{A} = \underline{K}^{-1}\ \underline{M} \tag{7}$$

Calculated eigenvalues and eigenmodes are used in the formation of control laws stated later.

4. General Damped Modal Analysis with Electrical Modelling and Gyroscopic Effect

A spring term and a damping term are the basic contents of the control input. However, as each element of the control system, sensor, compensation circuit, power amplifier, and control coil, has usually specific frequency characteristic, the complete PD (spring and damping) control is not realized. Therefore, an electrical modelling or a consideration of frequency characteristic is necessary. Also, gyroscopic effect should be taken into account for high speed rotors.

All these effects are included in the following formation.

Transfer function of control input against measured output ;

$$L(u/x)=(k_p+k_d s)\sum_i(a_i s^i)/\sum_i(b_i s^i) \tag{8}$$

where L( ) represents Laplace operation, k_p and k_d are gains of P and D control respectively, and a_i and b_i are coefficients of frequency characteristic, which is usually of a low pass filter (LPF) with gain decrease and phase lag at high frequency range.

In the case of 2nd order LPF with cutoff frequency f_c and Q value, equation (8) becomes ;

$$L(u/x)=(k_p+k_d s)/(1+b_1 s+b_2 s^2) \tag{8'}$$

$$b_1=1/Q/(2\pi f_c)\ ,\ b_2=1/(2\pi f_c)^2$$

Equation of motion with gyroscopic effect ;

$$\begin{aligned} m_k\ddot{x}_k &= F_{kx} - F_{kx}^* + u_{kx} && (9)\\ J_{rk}\ddot{\theta}_{yk} - J_{ak}\omega_r\dot{\theta}_{xk} &= M_{ky}^* - M_{ky} && (10)\\ m_k\ddot{y}_k &= F_{ky} - F_{ky}^* + u_{ky} && (11)\\ J_{rk}\ddot{\theta}_{xk} + J_{ak}\omega_r\dot{\theta}_{yk} &= M_{kx}^* - M_{kx} && (12)\end{aligned}$$

where ω_r is the angular rotational speed of the rotor, J_{ak} is the moment of inertia around the rotating axis and $J_{ak}\omega_r\dot{\theta}_k$ represents cross-coupling gyroscopic terms. θ_k in equation (4) is replaced by θ_{yk} in (10). (Refer Fig.2)

Define extended state vector ;

$$\underline{x}_e=(\underline{x}^T,\dot{\underline{x}}^T,\underline{u}_x{}^T,\dot{\underline{u}}_x{}^T,\underline{y}^T,\dot{\underline{y}}^T,\underline{u}_y{}^T,\dot{\underline{u}}_y{}^T)^T \tag{13}$$

$$\begin{aligned}\underline{x}&=(x_1,\theta_{y1},x_2,\theta_{y2},\cdots,x_{n+1},\theta_{y,n+1})^T\\ \underline{y}&=(y_1,\theta_{x1},y_2,\theta_{x2},\cdots,y_{n+1},\theta_{x,n+1})^T\\ \underline{u}_x&=(u_{x1},u_{x2},\cdots)^T\\ \underline{u}_y&=(u_{y1},u_{y2},\cdots)^T\end{aligned}$$

Extended equations of motion (9)-(12) are summarized as follows considering (8') and combining with an identity $\underline{M}\ \dot{\underline{x}}-\underline{M}\ \dot{\underline{x}}=\underline{0}$;

$$\underline{D}\ \dot{\underline{x}}_e + \underline{E}\ \underline{x}_e = \underline{0} \tag{14}$$

where

$$\underline{D} = \left[\begin{array}{c|c} \begin{matrix} \underline{0} & \underline{M} & \underline{0} \\ \underline{M} & \underline{0} & \underline{0} \\ \underline{0} & \{b_1\} & \{b_2\} \\ \underline{0} & \underline{I} & \underline{0} \end{matrix} & \underline{0} \\ \hline \underline{0} & \begin{matrix} \underline{0} & \underline{M} & \underline{0} \\ \underline{M} & \underline{0} & \underline{0} \\ \underline{0} & \{b_1\} & \{b_2\} \\ \underline{0} & \underline{I} & \underline{0} \end{matrix} \end{array}\right]$$

$$\underline{E} = \left[\begin{array}{c|c} \begin{matrix} \underline{K}_x & \underline{0} & -\underline{L} & \underline{0} \\ \underline{0} & -\underline{M} & \underline{0} & \underline{0} \\ -\underline{G}_{px} & -\underline{G}_{dx} & \underline{I} & \underline{0} \\ \underline{0} & \underline{0} & \underline{0} & -\underline{I} \end{matrix} & \begin{matrix} \underline{0} \quad -\underline{G}_{yro} \\ \hline \underline{0} \end{matrix} \\ \hline \begin{matrix} \underline{0} \quad +\underline{G}_{yro} \\ \hline \underline{0} \end{matrix} & \begin{matrix} \underline{K}_y & \underline{0} & -\underline{L} & \underline{0} \\ \underline{0} & -\underline{M} & \underline{0} & \underline{0} \\ -\underline{G}_{py} & -\underline{G}_{dy} & \underline{I} & \underline{0} \\ \underline{0} & \underline{0} & \underline{0} & -\underline{I} \end{matrix} \end{array}\right]$$

$$G_{yro}=\omega_r\cdot\mathrm{diag}\{0,J_{a1},0,J_{a2},\cdots,0,J_{a,n+1}\}$$

where $\underline{G}_p$ and $\underline{G}_d$ represents proportional and differential feed-back matrices containing k_p and k_d respectively and $\{b_i\}$ means diag$\{b_i\}$ or diagonal matrix representing filter characteristic of the control system. $\underline{I}$ is the unit matrix.

For this extended system, eigenvalue analysis can be performed similarly to equation (7) ;

$$\dot{\underline{x}}_e = \underline{A}_e\ \underline{x}_e \quad ; \quad \underline{A}_e = -\underline{D}^{-1}\underline{E} \tag{15}$$

As an eigenvalue analysis technique, QR method using Hessenberg matrix [6] has been employed here.

5. Experimental Apparatus

In order to investigate several control laws as practical design methods for the actual machines, an experimental apparatus was constructed as shown in Fig.3. A disk of weight 1.2Kg is mounted on the shaft of 410mm long and weight 2.2Kg with bearing diameter 40mm. The rotor is divided into 9 disks which have each mass and moment of inertia, with a resulting degree of freedom 36.

A small spring constant of 980 N/m was given to two bearings at ② and ⑦, and the undamped mode was analyzed with a condition nearly equal to free-free mode, the result of which is shown in Fig.4. 1st(1B) and 2nd(2B) eigenvalues of bending mode lie at 333 Hz and 633 Hz respectively, so this is a flexible rotor which passes critical speeds of bending modes before reaching the design rotational speed (50,000 rpm, 833 Hz). This result is also plotted on the imaginary axis of Fig.5. Between the two main bearings are mounted drive motor ④ and auxiliary bearing ⑤. The rotor displacements are measured at three points ③ ⑥ and ⑧.

6. Control laws

Rigid Mode Control

The rotor displacement at the center of gravity is estimated by polynomial curve fit using displacement sensor signals. For three sensors parabola approximation is performed. Neglecting bending modes of the rotor and assuming rigid body, PD control gains are obtained to give appropriate spring and damping to translational and rotational motion of the center of gravity.

With this control law damped eigenvalues are analyzed considering the rotor flexibility, and the result is plotted on Fig.5 with the symbol X. The 2nd bending mode of 627 Hz is unstable.

Pseudo-Inverse (PI)[2]

Let $\underline{T}$ be the modal matrix obtained by the undamped analysis, then using ;

$$\underline{x} = \underline{T}\,\underline{a} \quad \text{or} \quad \underline{a} = \underline{T}^{-1}\,\underline{x} \tag{16}$$

the equation of motion (6) is transformed into the following equation concerning the modal coordinate $\underline{a}$.

$$\underline{T}\,\underline{M}\,\underline{T}^{T}\,\ddot{\underline{a}} + \underline{T}^{T}\,\underline{K}\,\underline{T}\,\underline{a} = \underline{T}^{T}\,\underline{L}\,\underline{U} \tag{17}$$

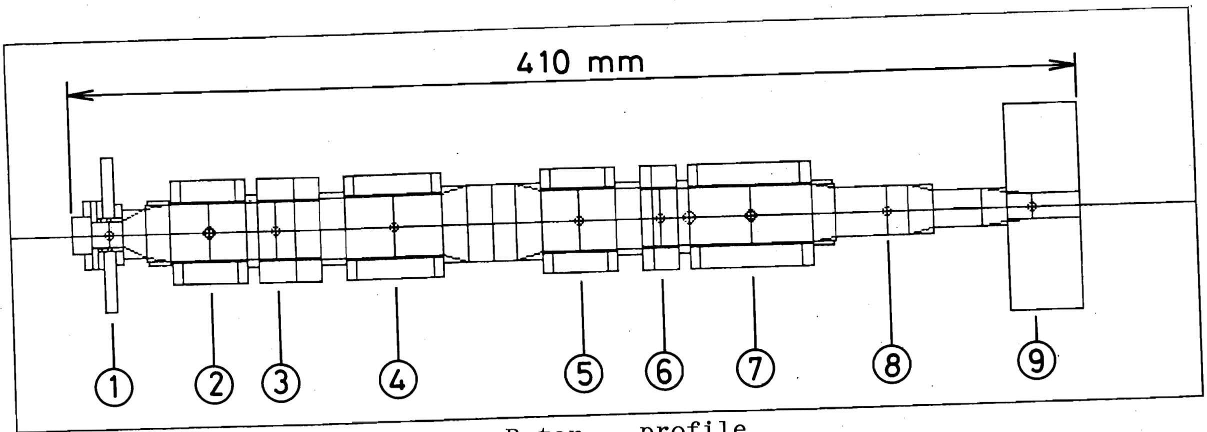

Figure 3 Rotor profile

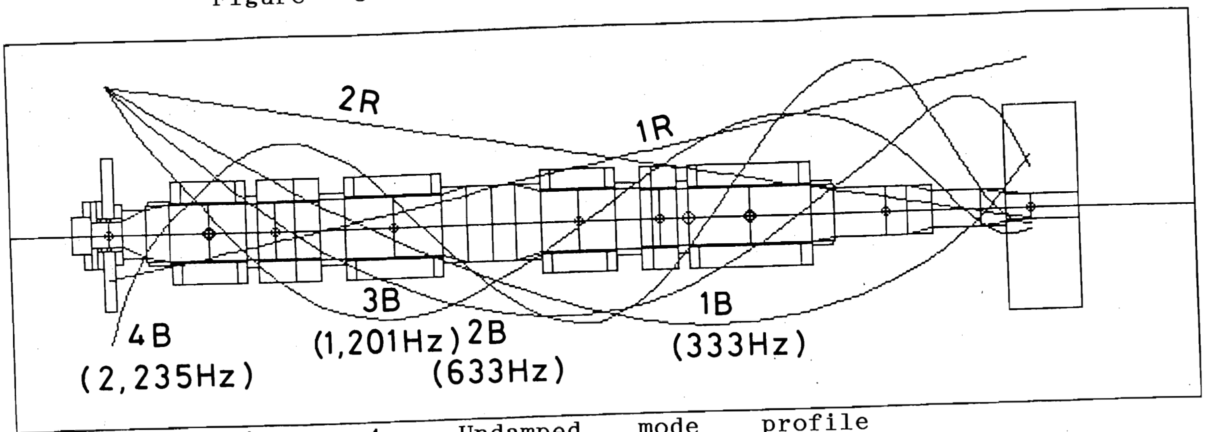

Figure 4 Undamped mode profile

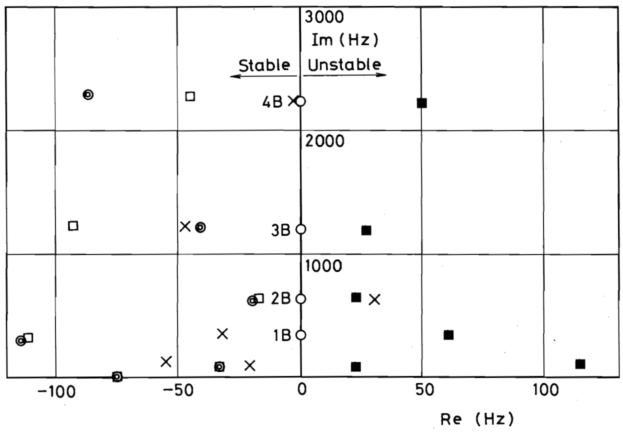

o : Undamped, free-free mode
x : Rigid mode
■ : Pseudo-Inverse, non-colocation
□ : Pseudo-Inverse, with colocation
◎ : Quasi-Colocation Pseudo-Inverse

Figure 5 Eigenvalues by various control laws

where

$$\underline{T}\ \underline{M}\ \underline{T}^T = \underline{I}$$
$$\underline{T}^T\ \underline{K}\ \underline{T} = \mathrm{diag}\{\omega_1{}^2, \omega_2{}^2, \cdots, \omega_n{}^2\}$$

Therefore, if the following control is realized ;

$$\underline{T}^T\ \underline{L}\ \underline{u} = \underline{F}\ \dot{\underline{a}}\ ;\ \underline{F} = \mathrm{diag}\{-2\xi_i\omega_i\} \quad (18)$$

then this is the ideal modal control which enables arbitrary selections of damping ratio ξ_i for the i-th mode with eigenfrequency ω_i. However, this is actually not realizable.

Let measured output of state $\underline{x}$ be $\underline{S}\ \underline{x}$ and the gain matrix of output velocity feed-back be $\underline{G}$, then

$$\underline{u} = \underline{G}\ \underline{S}\ \dot{\underline{x}} = \underline{G}\ \underline{S}\ \underline{T}\ \dot{\underline{a}} \quad (19)$$

Combining (18) with (19) ;

$$\underline{T}^T\ \underline{L}\ \underline{G}\ \underline{S}\ \underline{T} = \underline{F} \quad (20)$$

is the ideal relation of $\underline{G}$ and $\underline{F}$. However, (20) cannot be solved for $\underline{G}$, because $\underline{L}$ and $\underline{S}$ are not generally regular and square matrices.

Therefore, using Moore-Penrose's pseudo-inverse (indicated by #, see Appendix B) of $\underline{T}^T\ \underline{L}$ and $\underline{S}\ \underline{T}$;

$$\underline{G}_{PI} = (\underline{T}^T\ \underline{L})^{\#}\ \underline{F}\ (\underline{S}\ \underline{T})^{\#} \quad (21)$$

gives an approximated solution.

Eigenvalues calculated by PI method are plotted on Fig.5 with symbols ■. All the eigenvalues plotted are unstable. This is due to "non-colocation" condition that the locations of sensors and bearings differ each other. The importance of colocation condition is emphasized in [2].

Now suppose the case where colocation condition holds. Two sensors are located at points ② and ⑦ which correspond to those of two bearings. In this case the calculated eigenvalues are all stable with sufficient margins as seen from the plots of □ in Fig.5.

Thus PI method is very effective with the condition of colocation, while it is even worse in case of non-colocation, which is often the actual case.

Quasi-Colocation Pseudo-Inverse (QCPI)

In order to modify PI method for non-colocation case, displacement and velocity at the bearing location are estimated by polynomial curve fit using sensor signals as well as the case of rigid mode control. Then PI method is applied for the estimated states at the bearings.

Let measured states be $\underline{x}_m$, estimated states $\underline{x}_b$, and estimating matrix $\underline{E}_s$, then ;

$$\underline{x}_b = \underline{E}_s\ \underline{x}_m = \underline{E}_s\ \underline{S}\ \underline{x} \quad (22)$$
$$\underline{u} = \underline{G}\ \dot{\underline{x}}_b = \underline{G}\ \underline{E}_s\ \underline{S}\ \dot{\underline{x}} \quad (23)$$

$\underline{E}_s$ contains curve fitting informations which only depend on locations of each sensor and bearing. The feed-back matrix $\underline{G}$ is calculated as ;

$$\underline{G}_{QCPI} = (\underline{T}^T\ \underline{L})^{\#}\ \underline{F}\ (\underline{E}_s\ \underline{S}\ \underline{T})^{\#} \quad (24)$$

Calculated eigenvalues are shown on Fig.5 with symbols ◎. Eigenvalues of two rigid modes (1R,2R) and 1st(1B) and 2nd(2B) bending modes almost coincide with those of PI method with colocation condition. 3rd and 4th bending modes differ from colocation PI metod but still in the stable region. This means that modal shapes of the rotor of lower modes can sufficiently be approximated by a simple curve, in this case - parabola. The more increaes the number of sensors used, the higher mode shapes are well approximated and corresponding eigenvalues become stabler.

Selective Eigenvalue Move Method

QCPI method stated above has enabled basically stable arrangement of system eigenvalues. For the sake of safe passing of critical speeds or to cope with the change of eigenvalues due to gyroscopic effect at high rotational speed, it sometimes becomes necessary to move a specific eigenvalue towards stabler region. For this purpose, the following method is presented here.

The characteristic equation of a system of order n is ;

$$s^n+a_{n-1}s^{n-1}+\cdots+a_1s+a_0=0 \tag{25}$$

Consider following eigenvalue to move ;

$$s_k = s_{kr} \pm j\, s_{ki} \tag{26}$$

Equation (25) can also be expressed as ;

$$(s^{n-2}+b_{n-3}s^{n-3}+\cdots+b_1s+b_0) *(s^2-2s_{kr}s+s_{kr}^2+s_{ki}^2)=0 \tag{27}$$

a_i b_i and s_k are supposed to be all known. In order that s_k may change as;

$$s_k = (s_{kr}+\Delta s_{kr}) \pm j\,(s_{ki}+\Delta s_{ki}) \tag{28}$$

equation(25) changes correspondingly

$$s^n+(a_{n-1}+\Delta a_{n-1})s^{n-1}+\cdots +(a_1+\Delta a_1)s+a_0+\Delta a_0=0 \tag{29}$$

Also equation (27) changes into ;

$$(s^{n-2}+b_{n-3}s^{n-3}+\cdots+b_1s+b_0)*\{s^2-2(s_{kr}+\Delta s_{kr})s+(s_{kr}+\Delta s_{kr})^2+(s_{ki}+\Delta s_{ki})^2\}=0 \tag{30}$$

Therefore the increments of coefficients of the characteristic equation are ;

$$\Delta a_m=-2\Delta s_{kr}b_{m-1}+\Delta|s_k|^2b_m \quad (m=0,n-1) \tag{31}$$
$$\Delta|s_k|^2=(s_{kr}+\Delta s_{kr})^2+(s_{ki}+\Delta s_{ki})^2-s_{kr}^2-s_{ki}^2$$
$$b_{-1}\equiv0,\ b_{n-2}\equiv1,\ b_{n-1}\equiv0$$

Now feed-back gain $\underline{G}$ has to be considered to give Δa_m for specified Δs_{kr} and Δs_{ki}. The characteristic equation (25) is obtained from the system matrix $\underline{A}_e$ (15) as $\det|s\underline{I}-\underline{A}_e|=\underline{0}$. The effect of the change of elements in $\underline{G}$ included in $\underline{A}$ on eigenvalues or coefficients of (25) can be calculated actually conducting eigenvalue analysis. The element g_{ij} of $\underline{G}$ means the feed-back gain for i-th bearing from j-th sensor. Adding 1 to g_{ij}, coefficient increments $\underline{\Delta a}_{m,ij}$ (m=0, n-1) are obtained, and with these as column components a matrix $\underline{Z}_i$ is formed ;

$$\underline{Z}_i\ \underline{\Delta g}_i = \underline{\Delta a} \tag{32}$$

$$\underline{Z}_i=\{\underline{\Delta a}_{m,i1},\underline{\Delta a}_{m,i2},\cdots,\underline{\Delta a}_{m,ins}\}$$
$$\underline{\Delta a}_{m,ij}=\{\Delta a_{n-1,ij},\Delta a_{n-2,ij},\cdots,\Delta a_{0,ij}\}^T$$
$$\underline{\Delta g}_i=\{\Delta g_{i1},\Delta g_{i2},\cdots,\Delta g_{ins}\}^T$$
$$\underline{\Delta a}=\{\Delta a_{n-1},\Delta a_{n-2},\cdots,\Delta a_0\}^T$$

$\underline{\Delta g}_i$ is the increment of the feed-back gain g_{ij} and should be determined by (32). ns represents the number of sensors and is usually much less than the order of the system n. Therefore (32) cannot be solved strictly for $\underline{\Delta g}_i$. Thus the least square method is applied (see Appendix C). This is basically the same as using pseudo-inverse for column-regular matrix $\underline{Z}_i$. However, when the order of the system is large, each element of $\underline{\Delta a}$ differs by many figures, and the straight forward solution will result in a big error. Therefore each row of (32) is weighted inversely by binomial coefficients.

In the system basically stabilized by QCPI metod, the 2nd bending mode(2B) of 619 Hz has rather poor stability with damping ratio of 0.031. In order to stabilize this mode more, eigenvalue increment Δs_{2B} is specified and the resultant eigenvalues movement is plotted in Fig.6. For this actuator the auxiliary bearing ⑤ was used. It is ideal to move eigenvalue 2B only, but the actual approximation method allows small changes of other eigenvalues. 2B is certainly stabilized as larger values of negative Δs_{2B} are specified, while the second rigid mode (2R) is gradually deteriorated, also 1B turns towards unstable region from halfway. The point where the damping ratio of each eigenvalue approaches would be optimum.

The method stated above deals only one actuator(bearing). To deal plural actuators at the same time will make the equation corresponding to (32) non-

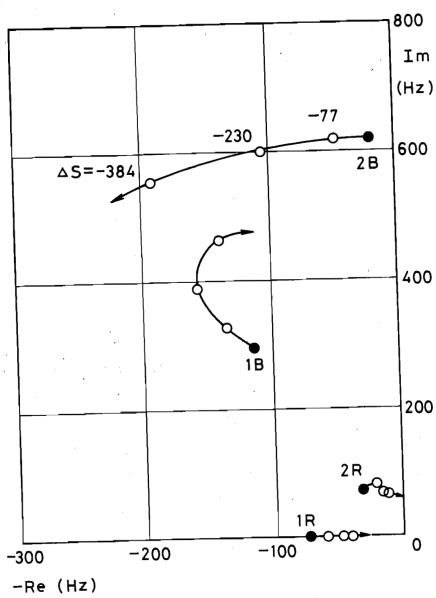

Figure 6 Selective Eigenvalue Move

linear and require iteration. It would be better to deal actuators one by one, watching the location of each eigenvalue and finally obtain the optimum feed-back gain.

7. Experimental Result

In order to test the actual system, a test signal is added to a point in the control system, and the response is measured at another point. The selection of these points is arbitrary, and the measuring point can even be the point located just before or after addition. Here the summing point is selected as input to the power amplifier of the horizontal (in y-direction) bearing ②, and the measuring point is the horizontal sensor ③. This can simulate the rotor displacement response to a disturbance force, which is expressed as $\underline{f}$ in the equation of motion (14) modified as ;

$$\underline{D}\,\dot{\underline{x}}_e + \underline{E}\,\underline{x}_e = \underline{f} \qquad (33)$$

The response transfer function is ;

$$L(\underline{x}_e/\underline{f})=(s\underline{I}-\underline{A}_e)^{-1}\underline{D}^{-1} \qquad (34)$$

The response of sensor ③ to the disturbance at bearing ② corresponds to one element of (34), which can be calculated numerically.

Fig.7 shows measured and calculated results in Bode diagram. The rotor is not rotating, so gyroscopic effect is not included. The calculated value of the broken line is of QCPI metod.

The peaks of 1.25 KHz and 2.25 KHz are due to rather small value of damping ratios of 3rd and 4th bending mode. These modes are actually self-oscillated due to more complicated frequncy characteristic than that of (8') and nonlinearity of the control components.

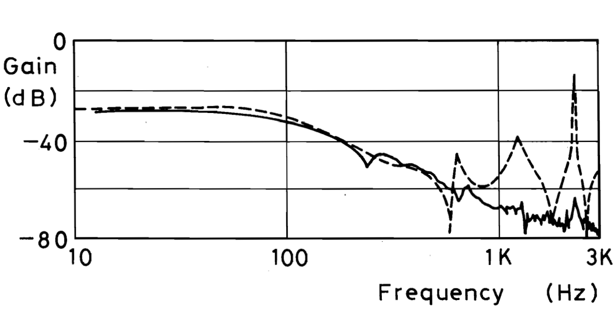

—— : Measured --- : Calculated

Figure 7 Frequency response

These oscillations were suppressed by using Notch filters, and the measured value of the real line in Fig.7 indicates the actual system response finally stabilized. In the lower frequency range, the measured characteristic is well simulated by the calculation indicating the effectiveness of the presented design method.

In the ralization of QCPI method, estimated displacement signals at the bearing are formed and input to the compensation circuit. It is an effective design rule to modify the compensation circuit watching the real system characteristic by the estimated signals[7].

8. Conclusion

(1) QCPI(Quasi-Colocation Pseudo-Inverse) method is effective for the basic design of flexible rotors.
(2) Selective Eigenvalue Move method works well for the fine modification of eigenvalues.
(3) The effectiveness of these techniques were proved experimentally.
(4) Finer modelling of the frequency characteristic of control components is necessary for the precise estimation at high frequency range.

References

[1] Nonami,K.,and Fleming D.P.:"QUASI-MODAL VIBRATION CONTROL BY MEANS OF ACTIVE CONTROL BEARINGS",Proc.Int. Conf. Rotordynamics, 1986,Tokyo
[2] Salm,J.R. "ACTIVE ELECTROMAGNETIC SUSPENSION OF AN ELASTIC ROTOR:MODELLING,CONTROL AND EXPERIMENTAL RESULTS" ASME DESIGN TECHNOLOGY CONFERENCES September,1987
[3] Chen,H.M., "Magnetic Bearings and Flexible Rotor Dynamics" STLE PREPRINT No.88-AM-2D-1
[4] Bradfield,C.D.,et.al. "A PROGRAMMABLE ELECTROMAGNETIC BEARING FOR VIBRATION CONTROL OF A FLEXIBLE SHAFT" ASME Vibration Conf. '89
[5] Burrows,C.R.,and Sahinkaya.M.N. "Control strategy for use with magnetic bearings" I.Mech.E. Int.Conf. on Vibrations in Rotating Machinery, September,1988
[6] Wilkinson,J.H., "The Algebraic Eigenvalue Problem" Oxford Science Publications
[7] Hisatani,M.,"Identification and Optimization of Active Magnetic Bearing Systems Using Measured Nyquist Diagrams" Proc.1st Int.Symp. Magnetic Bearings, June 1988

Appendix A Transfer Matrix of a shaft with variation of section

When there is no variation of section or no change in shaft diameter in Fig.2,

$$\begin{Bmatrix} F_{k+1} \\ M_{k+1} \\ \theta_{k+1} \\ x_{k+1} \end{Bmatrix} = \begin{bmatrix} 1 & 0 & 0 & 0 \\ l_k & 1 & 0 & 0 \\ l_k{}^2/2E_kI_k & l_k / E_kI_k & 1 & 0 \\ l_k{}^3/6E_kI_k & l_k{}^2/2E_kI_k & l_k & 1 \end{bmatrix} \begin{Bmatrix} F_k \\ M_k \\ \theta_k \\ x_k \end{Bmatrix}$$

This relation is expressed as

$$\underline{z}_{k+1} = \underline{T}_k \, \underline{z}_k$$

$\underline{T}_k$ is the transfer matrix of a shaft section with constant diameter. Now considering the variation of diameter, $\underline{T}_k$ is divided into several parts each representing a shaft section with constant diameter ;

$$\underline{T}_k = \underline{T}_{k,m} \, \underline{T}_{k,m-1} \cdots \underline{T}_{k,1}$$

Then this represents the transfer matrix of the whole shaft section with diameter variations which is used in equation (1).

Appendix B Moore-Penrose's Pseudo-Inverse [2]

For a column-regular matrix $\underline{B}$;

$$\underline{B}^{\#} = (\underline{B}^T\underline{B})^{-1}\,\underline{B}^T$$

For a row-regular matrix $\underline{C}$;

$$\underline{C}^{\#} = \underline{C}^T\,(\underline{C}\underline{C}^T)^{-1}$$

Appendix C Approximation by least square method

Consider the following simultaneous linear equations with the number of equations n larger than the number of unknowns n' ;

$$\sum_{j=1}^{n'} \alpha_{ij} x_j = b_i \qquad (\, i = 1,n \,)$$

Define the estimating function as ;

$$f = \sum_{k=1}^{n} \{(\sum_{j=1}^{n'} \alpha_{kj} x_j - b_k)/{}_nC_k\}^2$$

where ${}_nC_k$ is the binomial coefficient and ${}_nC_k = n!/(n-k)!k!$.
Then by partial differentiation ;

$$\partial f/\partial x_j = \sum_{k=1}^{n} 2\alpha_{kj} (\sum_{m=1}^{n'} \alpha_{km} x_m - b_k)/{}_nC_k = 0 \qquad (\, j = 1,n' \,)$$

Therefore the following equations concerning x_j are obtained ;

$$\{\sum_{k=1}^{n} \alpha_{ki}\alpha_{kj}/{}_nC_k\}\{x_j\} = \{\sum_{k=1}^{n} \alpha_{ki} b_k/{}_nC_k\} \qquad (\, i,j = 1,n' \,)$$